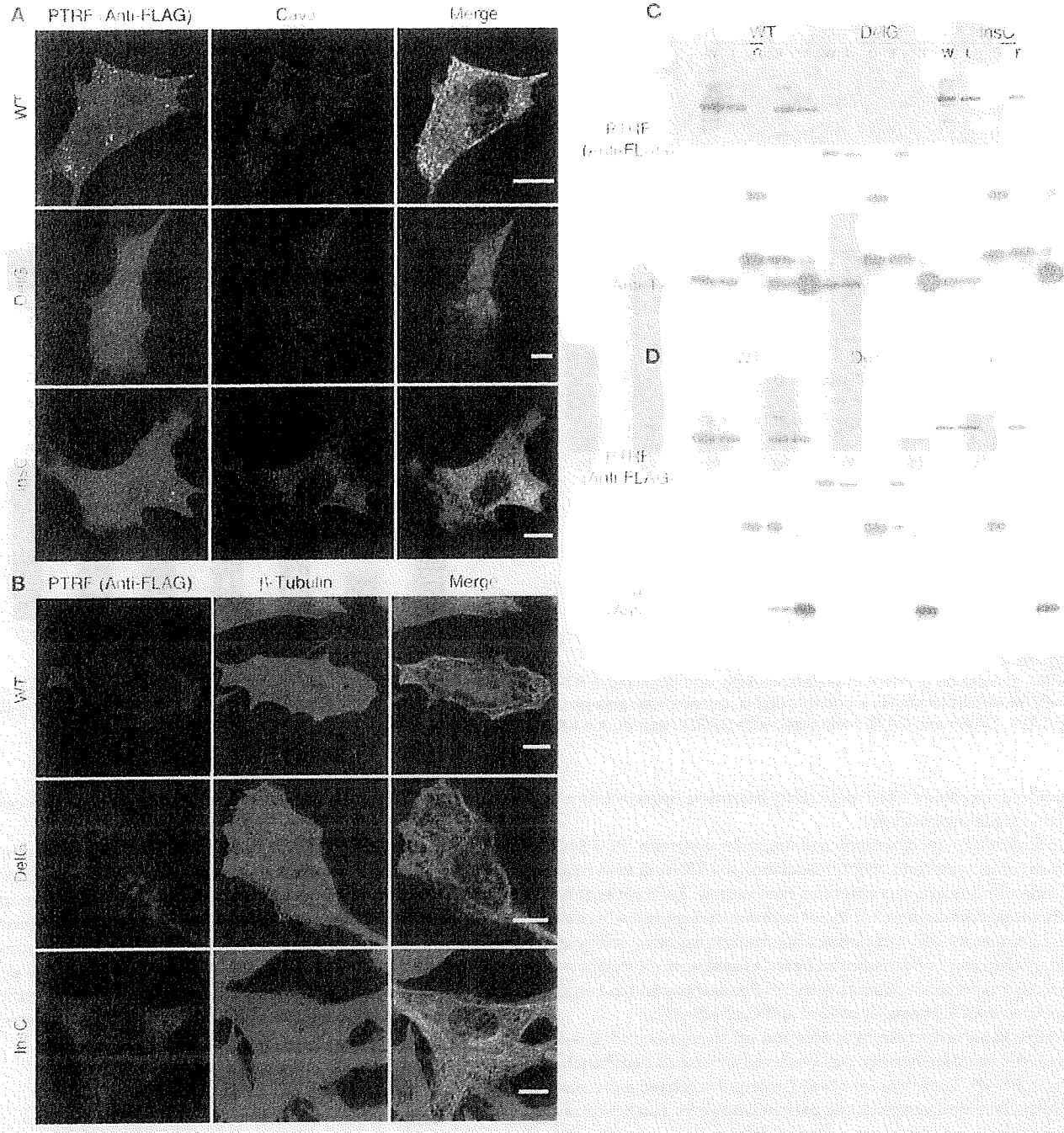

Figure 6
Altered localization of mutant PTRF in C2C12 cells and reduced binding ability to caveolins. C2C12 myoblasts were cotransfected with FLAG-tagged WT or mutant (c.525delG or c.696_697insC) PTRF cDNA and T7-tagged human caveolin-3. (**A** and **B**) WT PTRF stained by anti-FLAG antibody colocalized with caveolin-3 at the cell membrane. The deletion mutant accumulated in the nucleus, and the insertion mutant was seen in cytoplasm. (**A**) Membrane staining of caveolin-3 was decreased and was not colocalized with mutant PTRF. (**B**) The PTRF insertion mutant clearly colocalized with β-tubulin. Scale bars: 10 μm. (**C** and **D**) COS-7 cells were cotransfected with FLAG-tagged WT or mutant PTRF cDNA and T7-tagged human caveolin-3 (**C**) or caveolin-1 (**D**). The PTRF deletion mutant showed smaller molecular weight (estimated 30 kDa), and no immunoprecipitated protein was detected for FLAG or T7 antibodies. The PTRF insertion mutant showed slightly larger molecular weight, and amounts of coimmunoprecipitated proteins were greatly reduced. W, whole homogenate; L, cell lysate; G, control IgG; F, anti-FLAG; T, anti-T7.

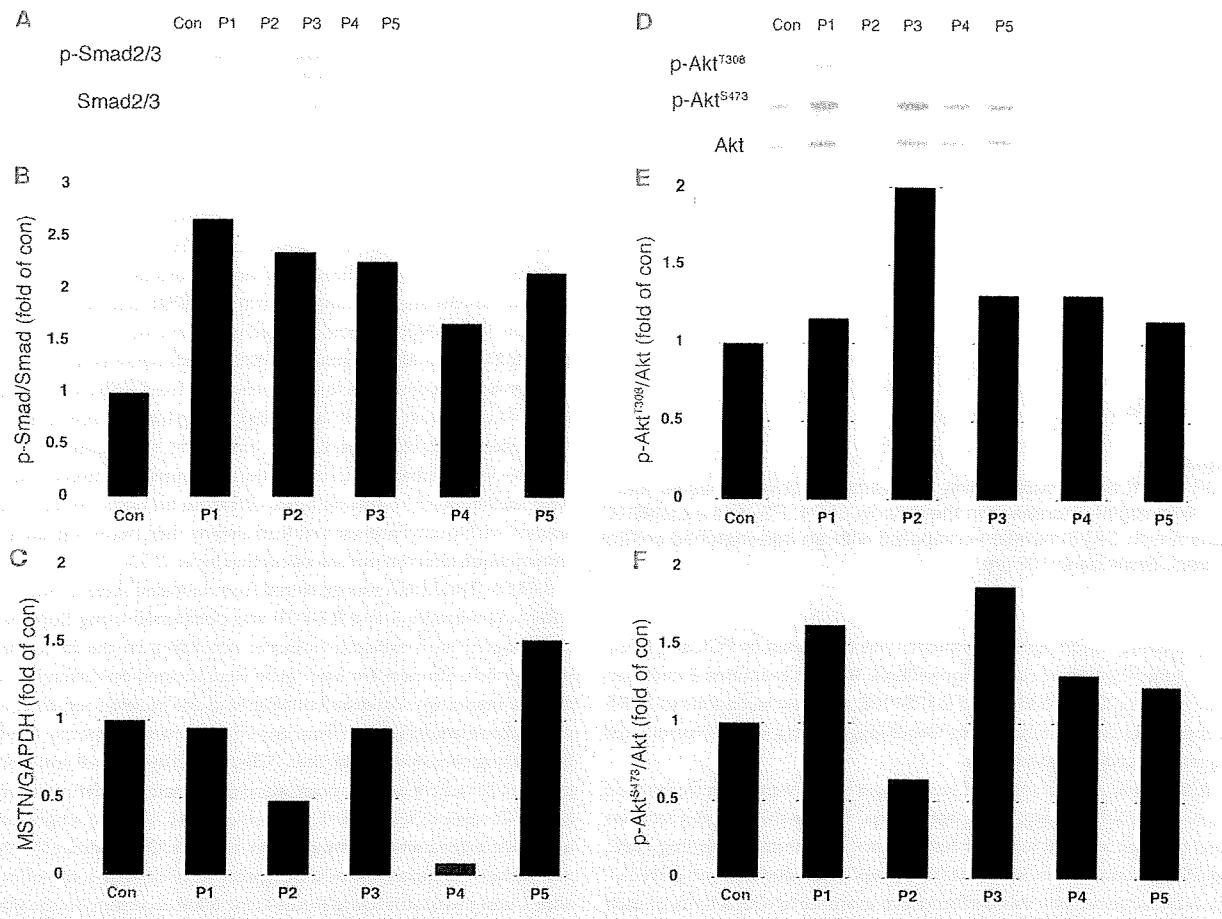

Figure 7
Increased p-Smad2 and p-Akt in P1–P5 skeletal muscle. (**A–C**) Immunoblotting analysis of Smad2/3 and p-Smad2/3$^{S423/425}$ (**A**) and densitometric analysis (**B**) showed increased p-Smad2/3 in P1–P5 compared with control muscle, with variable mRNA expression levels of myostatin (MSTN; **C**). (**D–F**) Immunoblotting analysis of p-Akt^{T308} and p-Akt^{S473}. Total Akt (**D**) and densitometric analysis (**E** and **F**) showed increased amounts of p-Akt in all patients except for p-Akt^{S473} in P2.

most clinical features observed in P1–P5 are likely to be explained by secondary reduction of caveolae and deficiency of caveolins.

Previously, Rajab et al. reported 10 of 17 patients with congenital generalized lipodystrophy unlinked to the loci of known CGL genes (37). The patients showed reduced exercise tolerance, percussion myoedema, cardiac hypertrophy, and arrhythmias. None of these patients had insulin resistance or early endocrine abnormalities (37). Ghanem also reported myoedema in a patient with Berardinelli-Seip lipodystrophy (38). Very recently, Simha et al. described CGL patients with muscle weakness and cervical spine instability (39). Because muscle involvement of these patients is similar to that of P1–P5 in the present study, *PTRF* mutations may not be rare in CGL patients.

This entity of generalized lipodystrophy with muscular dystrophy – which we believe to be novel – seems to represent a complicated disorder, as the occurrence of other symptoms could not readily be explained. Collection of detailed clinical information would therefore be essential in order to understand the precise function of PTRF.

Methods

Clinical materials. All clinical materials used in this study were obtained for diagnostic purposes and with informed consent. Subjects were selected from 2,745 muscular dystrophy specimens kept in the muscle repository of the National Center of Neurology and Psychiatry. The present studies were approved by the Ethical Committee at National Center of Neurology and Psychiatry.

Mutation screening and haplotype analysis. Genomic DNA was isolated from peripheral lymphocytes or muscles using standard techniques. All exons and their flanking intronic regions of *PTRF*, *CAV3*, *LMNA*, *AGPAT2*, *BSCL2*, *CAV1*, *PPARG*, *AKT2*, and *ZMPSTE24* were directly sequenced using genomic DNA from all patients using an ABI PRISM 3100 automated sequencer (Applied Biosystems). Primer sequences are listed in Supplemental Table 3. To confirm the compound heterozygosity in P5, the PCR product was cloned and sequenced. In order to determine the frequency of the mutations in *PTRF*, we performed enzyme digestion of PCR products from 200 Japanese control subjects using *Hpy*188III (New England Biolabs) for c.696_697insC and *Taq*I (New England Biolabs) for c.525delG. *Mbo*II (New England Biolabs) was used for enzyme digestion of PCR products to detect the c.1138G>A substitution in *BSCL2*.

For haplotype analysis, we used 6 SNPs (rs2062213, rs8070945, rs963988, rs963987, rs963986, and rs9252) within *PTRF*. PCR products were analyzed by direct sequencing or enzyme digestion using *Mae*III (Boehringer Mannheim). We also identified a novel 9-bp insertion polymorphism at the

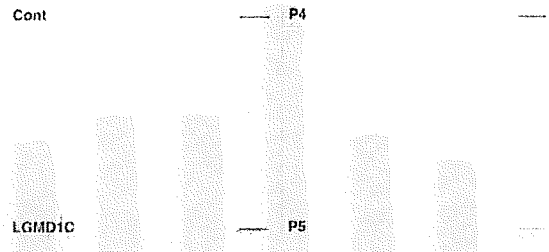

Figure 8
NDP activity assay. NDP activity was variable between muscle fibers, and was slightly increased in the muscle of P4, P5, and a LGMD1C patient with *CAV3* mutation compared with an age-matched control subject. Scale bars: 100 μm.

3′ noncoding region, and its frequency was calculated by PCR amplification using 50 Japanese control individuals. We also examined 2 microsatellite markers, STS-W93348 and D17S1185, the closest markers to *PTRF*. PCR product size was analyzed by GeneMapper using ABI 310 automated sequencer (Applied Biosystems).

Histochemical analysis. Biopsied muscle specimens were flash frozen with isopentane cooled in liquid nitrogen. Serial 10-μm-thick frozen sections were analyzed with 20 kinds of histochemical staining, including H&E, modified Gomori trichrome, NADH-tetrazolium reductase, and oil red O. The NDP activity assay was performed to examine nNOS activity of each muscle fiber, as described previously (40). In brief, 10-μm-thick frozen sections were fixed with 4% paraformaldehyde in PBS for 2 hours at 4°C. After a brief rinse with PBS, sections were incubated with 0.2% Triton X-100 in PBS for 20 minutes at 37°C. The reaction was performed for 1 hour in a dark, humidified chamber at 37°C in 0.2% Triton X-100, 0.2 mM NADPH, and 0.16 mg/ml nitro blue tetrazolium. The reaction was terminated by washing with water. We examined 6 age-matched controls and 2 LGMD1C patients with *CAV3* mutations (p.R27G and p.E33K).

Immunohistochemical analysis. Immunostaining was performed using standard methods. Serial 6-μm-thick frozen muscle sections were fixed in cold acetone for 5 minutes. After blocking with normal goat serum, sections were incubated with the primary antibodies for 2 hours at 37°C. We used antibodies against PTRF (A301-269A and A301-271A; BETHYL Laboratories), caveolin-1 (BD Biosciences), caveolin-2 (Sigma-Aldrich), caveolin-3 (BD Biosciences), and nNOS (BD Biosciences). Rabbit anti-PTRF antibody of A301-269A recognizes residue from 125 to 175, and A301-271A was raised against residue 238 and 288 of human PTRF (Figure 1B). In order to exclude other diagnosable muscular dystrophies, we used antibodies for dystrophin (DYS1, DYS2, and DYS3; Novocastra); α-, β-, γ-, and δ-sarcoglycans (Novocastra); α-dystroglycan (Upstate Biotech); β-dystroglycan (Novocastra); dysferlin (Novocastra); emerin (Novocastra); merosin (Chemicon); and collagen VI (ICN Biomedicals). After 6 rinses with PBS, sections were incubated with secondary antibodies of Alexa Fluor 488– or Alexa Fluor 568–labeled goat anti-mouse or -rabbit antibodies at room temperature for 45 minutes.

Immunoblotting analysis. Immunoblotting analysis was performed according to standard methods. Frozen muscle specimens were homogenized in SDS sample buffer and centrifuged at 15,000 *g* for 5 minutes. Protein (20 μg) from each sample was loaded on 12% SDS-polyacrylamide gels and transferred to PVDF membranes (Millipore). The membranes were blocked with 5% skim milk in PBS and immunoreacted with antibodies to PTRF (A301-269A and A301-271A), caveolin-2, caveolin-3, nNOS, Smad2/3 (Cell Signaling Technology), p-Smad2/3$^{S423/425}$ (Santa Cruz Biotechnology Inc.), Akt (Cell Signaling Technology), p-Akt^{T308} (Cell Signaling Technology), and p-Akt^{S473} (Cell Signaling Technology) overnight at 4°C. After washing in PBS containing 0.1% Tween-20, the membrane was incubated with horseradish peroxidase–labeled secondary antibody and visualized with ECL (Amersham Pharmacia Biotech). Data were analyzed using LAS-1000 chemiluminescence imaging system (Fujifilm). Quantification of immunoreactive bands was performed by densitometric analysis using Quantity One (PDI), and protein amounts for caveolin-3 and nNOS were normalized by the intensity of MHC. The ratio of p-Smad2/3 and p-Akt, to Smad and Akt, respectively, was also calculated.

Electron microscopy. Muscle specimens were fixed with 2% glutaraldehyde in 0.1 M cacodylate buffer. After shaking with a mixture of 4% osmium tetroxide, 1.5% lanthanum nitrate, and 0.2 M s-collidine for 2–3 hours, samples were embedded in epoxy resin. Semithin sections (1 μm thick) were stained with toluidine blue. Ultrathin sections 50 nm thick were stained with uranyl acetate and lead citrate, then examined under H-600 transmission electron microscope (Hitachi) at 75 kV.

RT-PCR. Total RNA was extracted from biopsied skeletal muscles using TRIzol (Invitrogen), and RT-PCR was performed using SuperScript III (Invitrogen) with random hexamer according to the manufacturer's instructions. Primers for each gene were located on different exons or directly spanning exon-exon boundaries of the genomic sequence in order to minimize amplification from any contaminating genomic DNA. After performing preliminary gradient PCR assays, the optimal annealing temperature for all the primer pairs was determined in order to generate the lowest Ct value as well as a sharp melting peak, with no amplification of nonspecific products or primer-dimer artifacts. Quantitative RT-PCR was performed to compare the mRNA expression of caveoin-1, caveolin-2, caveolin-3, and myostatin using Rotor-Gene 6000 according to the manufacturer's instructions (Corbett Life Science). The reactions were performed in reference to the GAPDH. We used 4 points consisting of 10-fold serial dilution using each primer set to build the standard curve. The PCR reaction (50 cycles) was followed by a melting curve analysis, ranging from 72°C to 95°C, with temperature increasing steps of 0.5°C every 10 seconds. Baseline and threshold values were automatically determined and analyzed. R^2 values exceeded 0.97. The 2–standard curve method was used to determine the relative expression ratio of the target gene in the patient samples versus the control sample, with reference to GAPDH expression.

Cell culture and transfection. COS-7 and C2C12 cells were maintained at 37°C in a humidified atmosphere of 5% CO_2 in DMEM (Sigma-Aldrich) supplemented with 10% fetal bovine serum. Full-length PTRF and caveolin-1 and -3 were amplified using total RNA from control human muscle and cloned into the pGEM-T-easy vector (Promega). The PTRF mutants c.525delG and c.696_697insC were generated using appropriate primers. All primer sequences are shown in Supplemental Table 3.

Immunocytochemistry. COS-7 and C2C12 myoblasts were cotransfected with FLAG-tagged WT or mutant (c.525delG or c.696_697insC) PTRF cDNA and T7-tagged human caveolin-3 using FuGENE6 (Roche). Transfectants were fixed for 30 minutes in 2% paraformaldehyde or 100% methanol, then permeabilized in 0.1% Triton X-100 for 10 minutes. Polyclonal antibodies to FLAG (Sigma-Aldrich) with caveolin-3 (BD Biosciences) or FLAG with β-tubulin (Calbiochem) were applied for double staining.

Immunoprecipitation. COS-7 cells were cotransfected with FLAG-tagged WT or mutant (c.525delG or c.696_697insC) PTRF cDNA and T7-tagged human caveolin-1 or caveolin-3 using FuGENE6 (Roche). The sequences of all constructs were verified with DNA sequencing using ABI PRISM 310 (Applied Biosystems). After 48 hours, the lysates from transfectants were

solubilized with 50 mM Tris-HCl (pH 7.5), 150 mM NaCl, 50 mM EDTA, 1% Triton X-100, and Complete-mini EDTA-free proteinase inhibitors (Roche) (9). The solubilized lysate precleared with Protein G Sepharose (GE Healthcare) was incubated with anti-FLAG (M2; Sigma-Aldrich) and anti-T7 (Novagen) antibodies. Immunoprecipitated proteins were dissociated from beads by boiling in sample buffer and were resolved by SDS-PAGE. Immunoblotting was performed using standard techniques.

Acknowledgments

We thank Sherine Shalaby (Heliopolis Neurocenter, Cairo, Egypt) and May Malicdan (National Center of Neurology and Psychiatry) for reviewing the manuscript. This study was supported by "Research on Psychiatric and Neurological Diseases and Mental Health" of "Health Labour Sciences Research Grant" and by "Research Grant (20B-12, 20B-13) for Nervous and Mental Disorders" from the Ministry of Health, Labor, and Welfare of Japan; by grants from the Human Frontier Science Program; by a Grant-in-Aid for Scientific Research from Japan Society for the Promotion of Science; by Research on Publicly Essential Drugs and Medical Devices from the Japanese Health Sciences Foundation; and by the Program for Promotion of Fundamental Studies in Health Sciences of the National Institute of Biomedical Innovation (NIBIO).

Received for publication January 20, 2009, and accepted in revised form June 3, 2009.

Address correspondence to: Yukiko K. Hayashi, Department of Neuromuscular Research, National Institute of Neuroscience, National Center of Neurology and Psychiatry, 4-1-1 Ogawa-higashi, Kodaira, 187-8502 Tokyo, Japan. Phone: 81-42-341-2711, Fax: 81-42-346-1742; E-mail: hayasi_y@ncnp.go.jp.

1. Scherer, P.E. et al. 1997. Cell-type and tissue-specific expression of caveolin-2. Caveolins 1 and 2 co-localize and form a stable hetero-oligomeric complex in vivo. *J. Biol. Chem.* **272**:29337–29346.
2. Tang, Z. et al. 1996. Molecular cloning of caveolin-3, a novel member of the caveolin gene family expressed predominantly in muscle. *J. Biol. Chem.* **271**:2255–2261.
3. Galbiati, F., Razani, B. and Lisanti, M.P. 2001. Emerging themes in lipid rafts and caveolae. *Cell.* **106**:403–411.
4. Thomas, C.M. and Smart, E.J. 2008. Caveolae structure and function. *J. Cell. Mol. Med.* **12**:796–809.
5. Hill, M.M., et al. 2008. PTRF-Cavin, a conserved cytoplasmic protein required for caveola formation and function. *Cell.* **132**:113–124.
6. Liu, L. et al. 2008. Deletion of Cavin/PTRF causes global loss of caveolae, dyslipidemia, and glucose intolerance. *Cell Metab.* **8**:310–317.
7. Minetti, C. et al. 1998. Mutations in the caveolin-3 gene cause autosomal dominant limb-girdle muscular dystrophy. *Nat. Genet.* **18**:365–368.
8. Matsuda, C., et al. 2001. The sarcolemmal proteins dysferlin and caveolin-3 interact in skeletal muscle. *Hum. Mol. Genet.* **10**:1761–1766.
9. Liu, L. and Pilch, P.F. 2008. A critical role of cavin (polymerase I and transcript release factor) in caveolae formation and organization. *J. Biol. Chem.* **283**:4314–4322.
10. Minetti, C. et al. 2002. Impairment of caveolae formation and T-system disorganization in human muscular dystrophy with caveolin-3 deficiency. *Am. J. Pathol.* **160**:265–270.
11. Ohsawa, Y. et al. 2006. Muscular atrophy of caveolin-3-deficient mice is rescued by myostatin inhibition. *J. Clin. Invest.* **116**:2924–2934.
12. Frost, R.A. and Lang, C.H. 2007. Protein kinase B/Akt: a nexus of growth factor and cytokine signaling in determining muscle mass. *J. Appl. Physiol.* **103**:378–387.
13. Venema, V.J., Ju, H., Zou, R., and Venema, R.C. 1997. Interaction of neuronal nitric-oxide synthase with caveolin-3 in skeletal muscle. Identification of a novel caveolin scaffolding/inhibitory domain. *J. Biol. Chem.* **272**:28187–28190.
14. Sunada, Y. et al. 2001. Transgenic mice expressing mutant caveolin-3 show severe myopathy associated with increased nNOS activity. *Hum. Mol. Genet.* **10**:173–178.
15. Agarwal, A.K., et al. 2002. AGPAT2 is mutated in congenital generalized lipodystrophy linked to chromosome 9q34. *Nat. Genet.* **31**:21–23.
16. Magre, J. et al. 2001. Identification of the gene altered in Berardinelli-Seip congenital lipodystrophy on chromosome 11q13. *Nat. Genet.* **28**:365–370.
17. Kim, C.A., et al. 2008. Association of a homozygous nonsense caveolin-1 mutation with Berardinelli-Seip congenital lipodystrophy. *J. Clin. Endocrinol. Metab.* **93**:1129–1134.
18. Cao, H. Alston, L. Ruschman, J. and Hegele, R.A. 2008. Heterozygous CAV1 frameshift mutations (MIM 601047) in patients with atypical partial lipodystrophy and hypertriglyceridemia. *Lipids Health Dis.* **7**:3.
19. Cao, H. and Hegele, R.A. 2000. Nuclear lamin A/C R482Q mutation in canadian kindreds with Dunnigan-type familial partial lipodystrophy. *Hum. Mol. Genet.* **9**:109–112.
20. Agarwal, A.K., et al. 2003. Phenotypic and genetic heterogeneity in congenital generalized lipodystrophy. *J. Clin. Endocrinol. Metab.* **88**:4840–4847.
21. George, S. et al. 2004. A family with severe insulin resistance and diabetes due to a mutation in AKT2. *Science.* **304**:1325–1328.
22. Barroso, I. et al. 1999. Dominant negative mutations in human PPARgamma associated with severe insulin resistance, diabetes mellitus and hypertension. *Nature.* **402**:880–883.
23. Hegele, R.A., et al. 2006. Sequencing of the reannotated LMNB2 gene reveals novel mutations in patients with acquired partial lipodystrophy. *Am. J. Hum. Genet.* **79**:383–389.
24. Aboulaich, N., Ortegren, U. Vener, A.V., and Stralfors, P. 2006. Association and insulin regulated translocation of hormone-sensitive lipase with PTRF. *Biochem. Biophys. Res. Commun.* **350**:657–661.
25. Razani, B., et al. 2002. Caveolin-1-deficient mice are lean, resistant to diet-induced obesity, and show hypertriglyceridemia with adipocyte abnormalities. *J. Biol. Chem.* **277**:8635–8647.
26. Fulizio, L. et al. 2005. Molecular and muscle pathology in a series of caveolinopathy patients. *Hum. Mutat.* **25**:82–89.
27. Betz, R.C. et al. 2001. Mutations in CAV3 cause mechanical hyperirritability of skeletal muscle in rippling muscle disease. *Nat. Genet.* **28**:218–219.
28. Sugie, K., et al. 2004. Two novel CAV3 gene mutations in Japanese families. *Neuromuscul. Disord.* **14**:810–814.
29. Hayashi, T. et al. 2004. Identification and functional analysis of a caveolin-3 mutation associated with familial hypertrophic cardiomyopathy. *Biochem. Biophys. Res. Commun.* **313**:178–184.
30. Vatta, M. et al. 2006. Mutant caveolin-3 induces persistent late sodium current and is associated with long-QT syndrome. *Circulation.* **114**:2104–2112.
31. Park, D.S., et al. 2002. Caveolin-1/3 double-knockout mice are viable, but lack both muscle and non-muscle caveolae, and develop a severe cardiomyopathic phenotype. *Am. J. Pathol.* **160**:2207–2217.
32. Woodman, S.E. et al. 2002. Caveolin-3 knock-out mice develop a progressive cardiomyopathy and show hyperactivation of the p42/44 MAPK cascade. *J. Biol. Chem.* **277**:38988–38997.
33. Zhao, Y.Y. et al. 2002. Defects in caveolin-1 cause dilated cardiomyopathy and pulmonary hypertension in knockout mice. *Proc. Natl. Acad. Sci. U. S. A.* **99**:11375–11380.
34. Xu, Y. Buikema, H. van Gilst, W.H. and Henning, R.H. 2008. Caveolae and endothelial dysfunction: filling the caves in cardiovascular disease. *Eur. J. Pharmacol.* **585**:256–260.
35. El-Yazbi, A.F. Cho, W.J., Boddy, G., and Daniel, E.E. 2005. Caveolin-1 gene knockout impairs nitrergic function in mouse small intestine. *Br. J. Pharmacol.* **145**:1017–1026.
36. Lobie, P.E. Sadir, R., Graichen, R. Mertani, H.C., and Morel, G. 1999. Caveolar internalization of growth hormone. *Exp. Cell Res.* **246**:47–55.
37. Rajab, A. Heathcote, K. Joshi, S. Jeffery, S. and Patton, M. 2002. Heterogeneity for congenital generalized lipodystrophy in seventeen patients from Oman. *Am. J. Med. Genet.* **110**:219–225.
38. Ghanem, Q. 1993. Percussion myoedema in a Pakistani boy with Berardinelli Seip lipodystrophy syndrome. *Clin. Genet.* **44**:277–278.
39. Simha, V. Agarwal, A.K. Aronin, P.A. Iannaccone, S.T. and Garg, A. 2008. Novel subtype of congenital generalized lipodystrophy associated with muscular weakness and cervical spine instability. *Am J. Med. Genet. A.* **146A**:2318–2326.
40. Kameya, S., et al. 1999. alpha1-syntrophin gene disruption results in the absence of neuronal-type nitric-oxide synthase at the sarcolemma but does not induce muscle degeneration. *J. Biol. Chem.* **274**:2193–2200.